

# Structure/Processing Relationships in the Fabrication of Nanoporous Gold

F. Kertis, J. Snyder, Lata Govada, Sahir Khurshid, N. Chayen, and J. Erlebacher

*Nanoporous gold made by dealloying silver/gold alloys is a relatively new material finding application in catalysis, sensing, and other areas. Here we discuss the metallurgical processing required to make patterned foils of nanoporous gold with large, flat grains, with which we are exploring an application as substrates for the heterogeneous nucleation of protein crystals.*

## INTRODUCTION

Figure 1 shows a scanning electron microscope (SEM) micrograph of a remarkable and beautiful material—nanoporous gold (NPG). Nanoporous gold can be a mesoporous or macroporous material, depending on whether we find its pore size in the 2–50 nm range (meso) or greater than 50 nm range (macro), following International Union of Pure and Applied Chemistry nomenclature.<sup>1,2</sup> It is being explored for a wide variety of applications that leverage its chemical inertness, ease of fabrication, high surface area, electrical conductivity, and flexible form factor. Such applications naturally include catalysis<sup>3–5</sup> and sensing,<sup>6</sup> but more unusual applications have been imagined. Perhaps NPG can be used as a support for enzymatic solar cells,<sup>7</sup> or as a substrate for the heterogeneous nucleation of macromolecule crystals (proteins) under milder supersaturation conditions than usually required.<sup>8</sup> The metallurgical development of NPG for the last of these applications motivates this article, and is discussed in more detail later.

The increase in research activity in NPG or dealloying (the electrochemical method used to make NPG), from ten papers in 2000 to 163 in 2009,<sup>9</sup> has been driven by two factors. First, NPG is an example of a bulk nanostructured

material. That is, the pores in NPG can be as small as 5 nm, but samples of NPG are themselves macroscopic. Having nanoscale features, NPG exhibits unusual optical and mechanical properties not associated with non-porous, bulk gold. For instance, it is brittle and very strong. It is not even gold colored, but instead can range in color from a deep reddish copper to nearly black (black gold!). The visceral nature of the material in the context of the explosion of interest in nanotechnology in the last decade should not be underestimated.

Second, the cultural history of NPG is fascinating. In the 20th century, deal-

loying and NPG were studied in the context of corrosion, as it is considered perhaps a model system for stress-corrosion cracking; that is, the focus was on how dealloying leads to materials degradation. A re-branding of dealloying as a useful materials processing tool has occurred over the last decade, but this is historically circular. Pre-Columbian artisans used dealloying to create so-called Tumbaga artworks, which used dealloying (aka “depletion gilding” to the art community) to create a golden skin over a base-metal enriched cast interior (see Figure 2),<sup>10</sup> and observations of the stability of gold alloys in various environments have been made periodically throughout the ages, such as Cennino Cennini’s admonition in the very first “how-to” book of art, dating from the early 15th century, that one should never use gold/silver alloy leaf outside, because it will turn black.<sup>11</sup>

The technique of dealloying to make nanoporous gold refers to the selective chemical or electrochemical dissolution of one alloy component from a multi-component metal.<sup>12</sup> Consider, for instance, the silver/gold alloy system. These components are completely miscible across the entire composition spectrum, a nearly ideal solution. However, if you immerse an Ag<sub>70</sub>Au<sub>30</sub> ingot into concentrated nitric acid, the silver will dissolve out, leaving behind NPG with a pore size of ~15 nm. This porous structure is much finer than the grain size of the original ingot, and the temptation would be to interpret the porosity as an excavated structure. This is not the case. Any number of diffraction tools would show a buried porous gold structure within the polycrystalline ingot, but none do. Rather, porosity forms dynamically during the dissolution of silver. As the silver atoms are

### How would you...

...describe the overall significance of this paper?

*Nanoporous gold has been receiving attention as a new bulk nanostructured material. Here we remedy the lack of processing information in the literature with a detailed review, and a discussion of the challenges found when tailoring the material to be a substrate for crystal growth from solution.*

...describe this work to a materials science and engineering professional with no experience in your technical specialty?

*We find that important bulk metallurgical principles must be applied to the fabrication, coarsening, and application of nanoporous gold, even though the feature size of the pores in this material is small compared to any grain size.*

...describe this work to a layperson?

*This paper describes how to make visible amounts of a nanostructured material, specifically, a porous metal whose feature sizes have nearly atomic dimensions.*

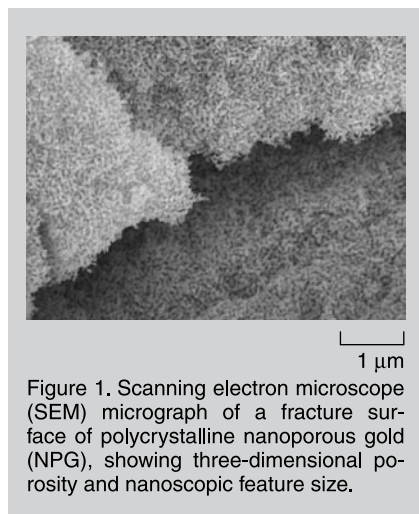


Figure 1. Scanning electron microscope (SEM) micrograph of a fracture surface of polycrystalline nanoporous gold (NPG), showing three-dimensional porosity and nanoscopic feature size.

being dissolved into the solution, the gold atoms that remain diffuse along the metal/electrolyte interface and reform into the porous structure.<sup>2,13</sup> What is particularly intriguing here is that the original lattice orientation of each grain is maintained. That is, the gold atoms are surface diffusing on the lattice of the underlying crystal and maintain the lattice. So, if one has a grain of Ag/Au 1 cm wide, it can be dealloyed to form a grain of NPG 1 cm wide. On the scale of porosity, grain boundaries are essentially absent.

The kinetics of dissolution and surface diffusion that are the elements of the choreography leading to porosity evolution have been discussed in a number of locations, and a working model has been developed that captures the essential aspects of the physics and chemistry of dealloying.<sup>1</sup> With the idea of a two-component random solid solution as the base alloy (e.g., silver/gold), the kinetics of dealloying are controlled mostly by the electrochemical potential placed on the alloy. Commonly, this potential is positive enough (on the hydrogen scale) that one component is oxidized to a soluble species, but the other is not.

Independent of materials, the characteristics of dealloying include an alloy parting limit,<sup>12</sup> a composition-dependent critical potential,<sup>14</sup> and a change in surface composition and morphology from planar to porous with increasing dissolution potential.<sup>12</sup> The parting limit refers to the sharp threshold in composition (% remaining component) above which dealloying cannot occur regardless of the applied potential. We

now understand the parting limit to be related to the geometry of percolation within the lattice, the central idea being that continuous chains of silver atoms of a certain width must exist if dissolution is to proceed into the bulk.<sup>15,16</sup> The critical potential  $E_c$  is that electrochemical potential required to actually dissolve silver from the lattice. Usually  $E_c$  is greater than the potential required to dissolve a pure material; for silver in silver/gold, the critical potential may rise hundreds of millivolts above the equilibrium potential of Ag/Ag<sup>+</sup>. We now understand the critical potential to be thermodynamic in origin, and is found by a free energy balance between the energy gained by dissolving silver into the solution, and the energy penalty associated with creating a new alloy/electrolyte interface.<sup>17</sup>

It is not surprising that the critical potential is often associated with the kinetic balance of silver dissolution rate and gold surface diffusivity, the latter being driven by capillary forces and tending to both smooth out and passivate the surface. Clearly, if gold diffusion is very fast compared to dissolution, then the surface will not corrode very deeply, behavior consistent



Figure 2. Columbian "tumbaga" sculpture ("Bell with Feline Deity") dated between 900–1500 A.D. Tumbaga refers to the gold/copper alloy used to make the artifact, which was then "depletion gilded" (i.e., surface dealloyed) to produce an object that looked like pure gold. Image permission of the Walters Art Gallery, Baltimore, Maryland.

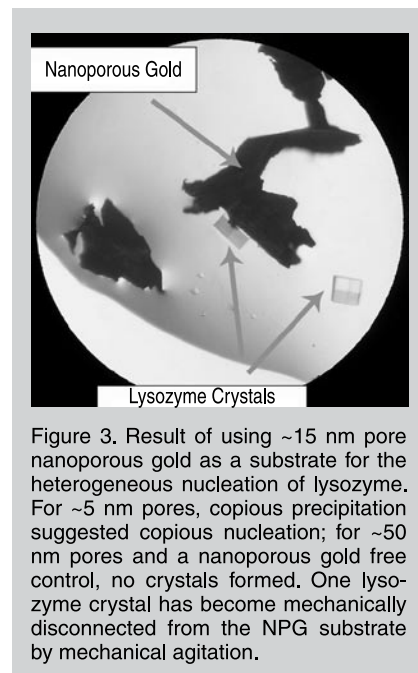
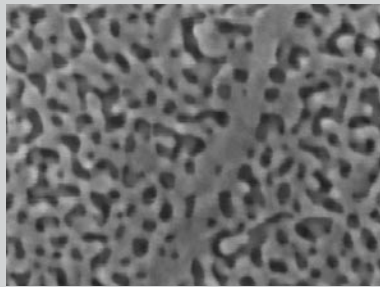


Figure 3. Result of using ~15 nm pore nanoporous gold as a substrate for the heterogeneous nucleation of lysozyme. For ~5 nm pores, copious precipitation suggested copious nucleation; for ~50 nm pores and a nanoporous gold free control, no crystals formed. One lysozyme crystal has become mechanically disconnected from the NPG substrate by mechanical agitation.

with dissolution at potentials below  $E_c$ . However, in practice, one must dealloy at a rate sufficiently high in order to grow nicely uniform, porous microstructures. This is an aspect of the distinction between an "intrinsic critical potential," that potential above which corrosion will occur, perhaps slowly and perhaps without porosity evolution, and the "empirical critical potential," which we would prefer be formally associated with porosity evolution.<sup>17,18</sup>

In this paper, we discuss some practical aspects of NPG fabrication. Our technology driver has been the formation of patterned, uniform and flat, highly porous surfaces with variable pore size with application as substrates for the nucleation and growth of macromolecules (proteins). The motivation for this project was an interesting observation that on porous substrates, with pore size of order the protein diameter, crystal nucleation occurred at milder supersaturations than typically required, leading to higher quality crystals (see Figure 3).<sup>8</sup> The increased nucleation rate with a porous substrate could be likened to homogeneous vs. heterogeneous nucleation during solidification, but with important differences. Primarily, the free energy of crystallization of a macromolecule is dominated by the change in entropy of the molecule as it changes from the fluid, random three-dimensional (3-D) phase, to a rigid, crystalline phase,<sup>19</sup>



10 nm

Figure 4. During recrystallization of NPG leaf, gold has segregated to grain boundaries to a high-enough concentration that they do not dealloy. This effect helps “zip” the grain boundary, as shown in the micrograph, and leads to good mechanical integrity.

and not by any enthalpic interaction with a substrate (indeed, a too-high interaction energy between proteins and surfaces tends to simply denature them). Our hypothesis has been that a random, porous substrate, allows the macromolecule to sample a quasi-random 3-D distribution of orientations near the surface, alleviating the entropic hit associated with nucleation.

The use of nanoporous gold for this application is natural, as the pore size is easily varied by annealing, and the surface chemistry of gold is easily modified by the use of adsorbing organic monolayers.<sup>20</sup> However, there are some important materials design constraints that needed to be overcome. The experiment called for small droplets of protein solution to be deposited on round patches of porous gold patterned on a foil of undealloyed material in the so-called “sitting drop” configuration. Macroscopic flatness (larger than the size of any protein or pore size) is not important here, but, as discussed below, we encountered unexpected metallurgical relationships between the grain size, rolling history and pore quality, and obstacles in patterning the substrates. Our experiences here may inform the utilization of NPG in other applications.

## METALLURGICAL PROCESSING OF NPG

### Initial Ingot Formation

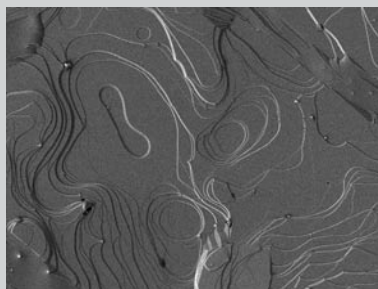
Alloy compositions from 20–40 at.% Au are suitable for dealloying to make NPG. More gold, and the parting

limit is passed; less gold and the material falls apart into a suspension of gold nanoparticles. Silver and gold form a homogenous solid solution across their entire composition range with a shallow two-phase region between the liquidus and solidus.<sup>21</sup> Silver and gold are both easily melted even in air, but one must be careful with silver-rich alloys as their melts possess high oxygen solubility and they tend to “volcano” when solidified. In the work presented here, alloys were melted in an induction furnace in a horizontal Bridgman-like configuration. The crucibles used were made of high purity graphite or a machinable alumina ceramic, with an ingot dimension of 0.25” × 0.25” × 1.5”. The packed crucible was placed in a quartz tube purged with flowing argon. The hot zone of the furnace coils was ~0.25” to 0.5” wide, depending on the RF power set on the induction furnace. The quartz tube was placed on two rollers. This configuration allowed translation of the crucible through the hot zone, a kind of crude hand-operated directional solidification.

Melting brings a race amount of



a



10 μm

Figure 5. (a) An example of a large grain (~5 cm wide) embedded in a silver/gold foil formed by the rolling annealing cycles described in the text. (b) SEM micrograph of the surface of the large grains showing wide flat terraces. Pinned step edges can be further minimized using the cleaning protocols described in the text.

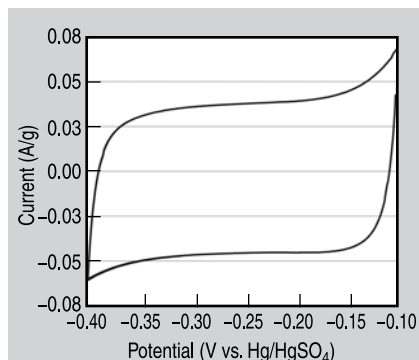


Figure 6. Electrochemical double layer capacitance measurement of clean, oxide-free NPG. Scan rate 5 mV/s, 0.1 M H<sub>2</sub>SO<sub>4</sub>.

buried oxide or carbide to the surface, which could be pulled off to the side and ground off after solidification. These impurities impeded grain growth (see below), and were important to remove completely. They exist even with high purity (greater than 99.99% pure) starting materials. Often, a dozen or more solidification/cleaning cycles were required to get a clean melt. Homogenization of the solidified ingots was performed at temperatures between 850 and 900°C for periods greater than 24 h.

After solidification, ceramic dust from the furnace impeded the formation of clear step trains and flat terraces on the surface of the crystals. A cleaning protocol of 5 minutes in an oxygen plasma cleaner followed by immersion in saturated NaOH solution at 200°C removed carbide or carbon impurities, and the NaOH solution alone dissolved surface oxide impurities.

### Fabrication of Large Grain Silver/Gold Alloy Foil

Under the right processing conditions, NPG, or more generally nanoporous metals made by dealloying, retain the same polycrystalline microstructure as their parent alloy. The surface diffusion mass transport leading to porosity evolution in principle occurs only on the lattice of the grains, so if one started with a grain size of 10 μm, then one would be left with NPG with 10 μm grains, even though the pore size may be only 10 nm. This characteristic has led to NPG being processed in many different forms. A survey of these forms include bulk samples of order a few millimeters wide,<sup>22</sup> nanowires,<sup>23</sup>

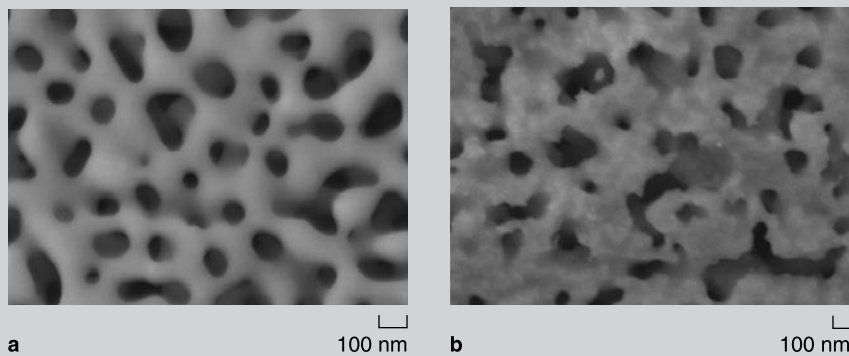


Figure 7. An extreme example of how surface reduction can affect thermal coarsening of NPG. Samples were from the sample batch, dealloyed in 0.1 M  $\text{AgNO}_3$  and annealed at  $600^\circ\text{C}$  for 5 minutes; there is a residual 15% silver content. (a) Residual surface oxide was reduced at  $-0.4$  V vs.  $\text{Hg}/\text{HgSO}_4$  until the reduction current dropped to zero. (b) No reduction.

vapor-deposited and micromachined thin films,<sup>24,25</sup> rolled foils,<sup>26</sup> and even free-standing hammered ultra-thin foils commonly called “leaf.”<sup>27</sup>

It was in the context of studying gold leaf that some metallurgical relationships between the grain structure and NPG quality became clear. Previously, it has been noticed in the context of studies of stress-corrosion cracking that in an ingot of silver/gold that was solidified and then homogenized, silver tended to segregate to the grain boundaries.<sup>28</sup> Upon dealloying, this led

to some grain boundary cracking, an effect that needed to be deconvoluted from the mechanical properties of NPG itself. In extreme cases, such segregation and cracking has been used to facilitate the formation of films of NPG “prisms.”<sup>29</sup> (As an aside, the mechanical properties of NPG is an interesting sub-field, focused on the mechanics of nanoscale truss systems whose characteristic lengths are smaller than any dislocation cell size.<sup>30</sup> Nanoporous gold with pore sizes less than  $\sim 50$  nm are inherently brittle,<sup>31</sup> even though gold is

ductile, for reasons that are unclear but whose elucidation may have important ramifications for understanding stress corrosion cracking of engineering alloys).

When NPG leaf (original alloy composition  $\text{Ag}_{65}\text{Au}_{35}$ ) was examined, it was noticed that although the hammered foil was only 100–150 nm thick, that lateral grain size often exceeded  $10\ \mu\text{m}$ .<sup>27</sup> As there is no annealing step in the fabrication of leaf, this observation strongly suggested room-temperature recrystallization had occurred. But equally interesting, Scanning electron microscopy (SEM) observation of the grain boundaries in the dealloyed microstructure showed they were gold-rich (Figure 4). The observation suggested that recrystallization leads to segregation and enrichment of gold at grain boundaries, which tends to “zip up” the microstructure upon dealloying.<sup>26,27</sup>

In our application as substrates for crystal growth, minimization of grain boundary cracking is obviously important. Ideally, as well, the grain size would be larger than the droplet of solution from which the proteins precipitate (3 mm). While the observations

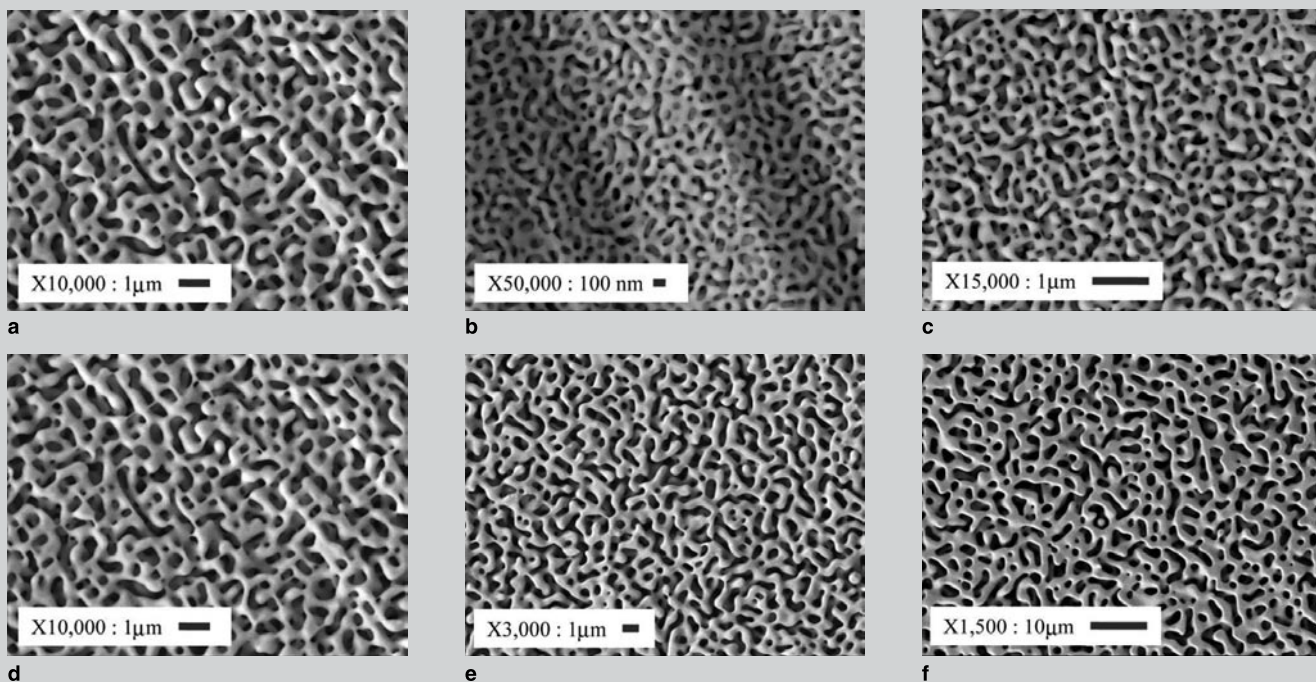


Figure 8. Scanning electron microscopy micrographs of samples of NPG annealed at various times and temperatures. Note the striking self-similar aspect to the coarsening, the topographic features of the precursor alloy surface (e.g., the ridges in the  $300^\circ\text{C}$  sample), and how the crystallographic orientation of the grains are manifested in the porous structure (e.g., local two-fold symmetry in the (001)  $600^\circ\text{C}$  sample, and local three-fold symmetry in the  $900^\circ\text{C}$  sample). (a) As-dealloyed in concentrated nitric acid; (b)  $300^\circ\text{C}$ , 15 min.; (c)  $400^\circ\text{C}$ , 15 min.; (d)  $600^\circ\text{C}$ , 5 min. (note scale change); (e)  $800^\circ\text{C}$ , 10 min.; (f)  $900^\circ\text{C}$ , 30 min.

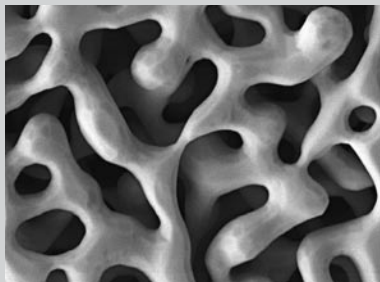


Figure 9. Faceted NPG, made by annealing at 600°C for 24 h followed by a slow cooling to 375°C.

of gold segregation to grain boundaries in leaf was suggestive, 10 μm was too small. Vapor-deposited films were unsuitable for this application because the grain size tended to be small compared to the length scale of porosity, and thin film deposition stresses tend to lead to cracking and delamination upon dealloying.<sup>24</sup> It was decided that a useful substrate form factor would be rolled foils, and a rolling and annealing protocol was developed to generate the required large grains; the grain size sometimes exceeded 2 cm laterally. The method is a variation on the technique sometimes referred to as critical strain annealing.

Critical strain annealing (CSA) is premised on the notion there is a critical strain which must be surpassed before which a sample will recrystallize upon annealing.<sup>32</sup> Furthermore, the more one strains above the critical strain, the more grains will appear upon recrystallization. Usually, this is explained by a nucleation argument—the more plastic strain induced in the sample, the more nucleation of stress-free grains upon recrystallization. Central to the argument is the unstated notion that the stress drives not only nucleation, but also grain growth. For silver/gold alloys, we find the CSA to be ~1%; however, even with highly pure samples, there is still copious nucleation, and the typical lateral grain size of as-rolled and recrystallized samples is less than 100 μm.

In foils rolled to a thickness less than 100 μm, many of the recrystallized grains are columnar, and some of them even have the low-energy (111) surface orientations (which is neither the rolling nor the recrystallization

texture). We have found that if foils less than 100 μm are rolled to strains *less* than the CSA, and then annealed again, grain growth occurs without recrystallization. Serendipitously, the (111) oriented grains grow fastest. Furthermore, this process can be repeated to get large grains; order cm lateral dimension grains are shown in Figure 5. Microscopically, these grains have extremely flat surfaces, with wide terraces often exceeding 100 μm,<sup>33</sup> and the slight gold segregation to grain boundaries that keeps the samples “zipped” during dealloying. Interestingly, this grain growth requires rolling, and we have not been able to induce grain growth by tension. The working hypothesis here is that the columnar grain boundaries need to be put in shear in order to de-pin them, as suggested by Cahn.<sup>34</sup>

The details of the processing used to grow large, flat grains in rolled thin foils are as follows. A clean, homogenized ingot of silver/gold is rolled to a thickness less than 100 μm. The foil is cut into sheets and stacked between machinable alumina plates, and annealed for 24 hours at 900°C. Stacking of the foils between ceramic plates is important to keep a high vapor pressure atmosphere of silver around the sample; otherwise the surface tends to lose silver due to evaporation and drops in composition below the parting limit. The first anneal leads to recrystallization. After the first anneal, the foils are lightly rolled either between

smooth tungsten foil or between sheets of smooth acrylic, but only so that there is a slight smoothing of the surface. Then, samples are re-annealed at 900°C, again stacked between ceramic plates. This light rolling/annealing cycle is repeated (usually 5–6 times) until the desired grain size is achieved.

### Dealloying Silver/Gold to Make NPG

In dealloying (i.e., the actual formation of porosity), two concerns are paramount: pore/ligament size (morphology) and residual silver fraction (composition). During the initial dissolution process, the pore size can be controlled a bit by the initial alloy composition. Alloys with lower gold fraction tend to have larger pores, and alloys with gold fractions nearer to the parting limit composition tend to have smaller pores, although there have been no systematic studies.

The most common method to dealloy silver from silver/gold alloys is by immersion in concentrated nitric acid, in which silver is highly soluble. This condition is called “free corrosion.” While surface diffusion of gold is required to form the porous structure, the nature of the surface species that participates in surface diffusion is highly dependent on the anion in the electrolyte, because each kind of anion forms a complex with diffusing gold atoms that has a different binding energy. This is an important point, and leads to the observation that the chemical

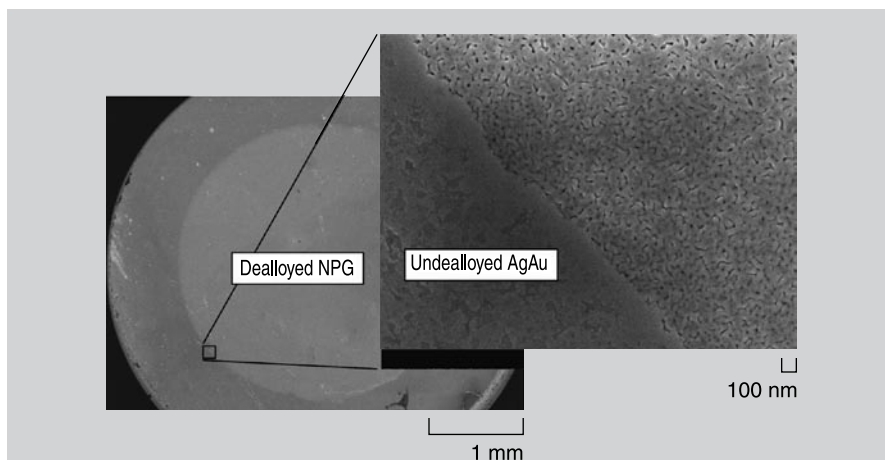


Figure 10. Scanning electron microscopy images of a single crystal grain in a Ag/Au foil with a 2 mm diameter patterned region of NPG made with a PDMS mask. Dealloying was performed in 0.1 M AgNO<sub>3</sub> at 0.563 V vs. Hg/HgSO<sub>4</sub> for 10 minutes, then the sample was reduced in 0.1 M H<sub>2</sub>SO<sub>4</sub> at -0.1 V vs. Hg/HgSO<sub>4</sub>, and annealed at 400°C for 30 minutes to accentuate the porous region at lower magnifications.

composition of the electrolyte leads to different gold surface diffusion rates. Most anions that complex  $\text{Ag}^+$  into a soluble species lead to orders-of-magnitude increases in the surface diffusivity of gold compared to vacuum or aqueous conditions without any ionic species.<sup>35</sup>

At room temperature, anions such as nitrate lead to pore sizes in the 10–15 nm range during the initial stages of dealloying, but if the sample is left in nitric for periods of about 24 hours, this pore size coarsens to ~30 nm.<sup>27</sup> Smaller pore sizes in nitric can be made if the nitric acid is cooled to  $-20^\circ\text{C}$ .<sup>36</sup> The addition of chloride, bromide, or iodide to the dealloying electrolyte leads to large increases in the surface diffusivity of gold, and consequently porosity with larger feature sizes.<sup>37</sup> One must be careful with the use of these anions, however—a too-high concentration of chloride leads to the formation of insoluble silver chloride species on the surface, and all of these anions are difficult to fully desorb.

For better control of the pore size during dealloying, a potentiostat in a three electrode configuration is used. The advantage here is that milder acids can be used, and there is better control over pore morphology. (The nature of the reference electrode is important and chloride from common  $\text{Ag}/\text{AgCl}$  reference electrodes can contaminate the electrolyte; use a salt bridge, or, preferably, a  $\text{Hg}/\text{HgSO}_4$  reference.) The higher the dealloying potential (above the critical potential), the faster silver dissolution proceeds compared to gold surface diffusion, and the finer the porosity. Here, the concern is that at high potentials surface oxide species can form. The nature of these surface species have not been fully clarified, although there are reports of gold oxide formation.<sup>38</sup>

An especially benign and easy method to make highly porous NPG is to dealloy in neutral silver nitrate, e.g., 0.1  $\text{AgNO}_3$  at high potential. As discussed in Reference 39, the use of a neutral solution is non-intuitive because the Pourbaix (potential/pH/phase) diagram suggests that at high anodic potentials silver will form insoluble oxides. However, once the instability initiates, there is an accumulation of protons right at

the etch front, creating a pH depression at the etch front. This situation is analogous to mechanisms of pitting or crevice corrosion. What's convenient is that immediately behind the etch front, the pH rises, leading to the formation of a morphology-stabilizing surface oxide. In this way, pore sizes as small as 5 nm are easily formed at room temperature. The flipside to the morphological stabilization is a significant amount of residual silver remains in the final sample of NPG, which can be as high as 15%. This silver can be removed, however, by repeated reduction/dissolution cycles.<sup>39</sup>

We find that regardless of electrolyte and dealloying potential, significant amounts of residual surface oxide species of some sort always remain. These can be reduced in dilute sulfuric acid, and such reduction is important for clean surface electrochemistry, or for reproducible thermal anneals. Figure 6 shows cyclic voltammograms in the double layer region of a sample of NPG dealloyed in silver nitrate. The square, symmetric character of the voltammograms is a good check on the quality of the material, and will not be found on samples with any degree of surface oxide (the slight vertical offset disappears in deaerated electrolyte). It is interesting to note that for these samples we measure a specific capacitance of 11 F/g. On a mass basis, this is low, but on an atom basis the capacitance is ~2,100 F/mol, approximately the same as carbon nanotubes.<sup>40</sup>

### Annealing of NPG

The pore size of NPG can be further processed by thermal annealing, in order to grow the pore/ligament size to scales upwards of 10  $\mu\text{m}$ . Here, it is quite important to thoroughly clean any electrolyte off the sample, and start with a fully reduced surface. Figure 7 shows an example of annealed NPG with and without residual surface oxide. The bumpy, sharp features of the sample annealed without reduction have clearly inhibited coarsening and led to a more random, bumpy, and finer scale material. Examples of porous gold with such features are commonly found in the literature,<sup>41</sup> and coarsening results from such samples should be viewed with caution.<sup>42</sup>

Figure 8 shows examples of clean NPG annealed at various temperatures and times. The pores in the bottom right of Figure 8, annealed at  $900^\circ\text{C}$  for 30 minutes, are large enough to be seen with optical microscopy. For many of these samples, the crystallographic orientation of the underlying grain is readily apparent in the quasi-random periodicity or symmetry of the final material. The three-fold symmetry of the (111) oriented grains are apparent in the 120 degree angles (Figure 8, bottom right), and on (001) oriented grains (Figure 8, bottom left) cubic symmetry is apparent. High resolution transmission electron microscopy (TEM) confirms the single-crystal nature of this material, if it wasn't obvious from the grain observations.<sup>27</sup> In microscopy, however, one must be careful about sample preparation. Ion milling for sample thinning or focused ion beam milling tends to break up the ligaments into polycrystalline aggregates; although the resultant materials are porous, they are not indicative of the native microstructure. This has been a point of confusion for some groups in the recent literature,<sup>41,43,44</sup> but hopefully a recent x-ray diffraction and orientational imaging microscopy study have now resolved single crystal nature of NPG once and for all.<sup>44</sup>

An interesting morphological characteristic of the annealed samples in Figure 8 is that there is a pronounced lack of facets. This observation is a result of processing and surface thermodynamics. Scanning electron microscopy of small gold particles<sup>45</sup> has shown that the equilibrium, or Wulff shape of gold crystallites is not fully faceted at high temperatures. At  $1,000^\circ\text{C}$ , most of the surface area of the equilibrium shape is actually completely round, with only small (111) facets. We hypothesize that an analogous situation is the case for all of the samples in Figure 8, which have been quenched quickly by taking small samples out of hot furnaces. In Figure 9, a sample placed in a hot  $600^\circ\text{C}$  furnace, and then slowly cooled to  $<400^\circ\text{C}$  is shown, and here the length scale and kinetics have led to nicely faceted ligaments.

To reiterate an earlier point, the nice, extended porous microstructure in annealed NPG is only apparent because

the grain size is always bigger than the pore size by at least an order of magnitude. Materials with small grain sizes can also be dealloyed, but if both the pore and grain size is of the order of nanometers, the final product tends to be a porous sintered agglomeration of nanoparticles, and not NPG. This is an important distinction here because the properties of the sintered agglomerate are dominated by grain boundaries. These properties include the mechanical properties, but also thermal stability. In well-prepared NPG, there are no grain boundaries, and thus no grain boundary grooving. Grain boundaries are unstable to thermal grooving, and such materials tend to coarsen driven by chemical potential gradients associated with the local (positive) spherical curvature of the grains (as in models of grain growth or Ostwald ripening). In contrast, ligaments in NPG are morphological saddle points, with both positive and negative curvature. The inclusion of the negative curvature term in the chemical potential given by the Gibbs-Thomson equation alleviates the chemical potential gradient, leading to greater morphological stability.<sup>46</sup>

### Patterning NPG

The particular goal we have been concerned with here is the production of clearly delineated circles of NPG on silver/gold foil with as large grains as possible/convenient. For this purpose a mask is required, and the common polydimethylsiloxane (PDMS) elastomer used in so-called “soft lithography” works well for this purpose. Polydimethylsiloxane, however, is not very stable in strong acids, which also tend to seep into the elastomer/metal interface, and thus dealloying in concentrated nitric acid under free corrosion is not an option. With these observations in mind, we have found our best patterning results by using a PDMS mask that is not fully cured, and silver nitrate as a dealloying electrolyte. Figure 10 shows an example of our success—a circular patterned region of NPG.

## CONCLUSIONS

The history of NPG began by studying it as a prototypical material for corrosion—a materials degradation process with negative connotation. Over the last decade, the material has been considered as useful and applicable in its own right. And more generally, dealloying is being considered a flexible and important processing tool to make bulk amounts of nanostructured materials. The authors are continually surprised by the further observation that classical metallurgy involving problems such as grain growth, recrystallization, texture development, surface orientation, Wulff shape, etc., plays such a central role in the fabrication of high quality material.

## ACKNOWLEDGEMENTS

*The authors are grateful to the U.S. National Science Foundation (NSF) and the U.K. Engineering and Physical Sciences Research Council via a Materials World Network program funded under grants DMR-0804187 (NSF) and the EP/G027005 (EPSRC).*

## References

1. J. Erlebacher and R. Seshadri, *MRS Bulletin*, 34 (2009), pp. 561–566.
2. J. Erlebacher et al., *Nature*, 410 (2001), pp. 450–453.
3. Y. Ding and M.W. Chen, *MRS Bulletin*, 34 (2009), pp. 569–576.
4. C. Xu et al., *J. Am. Chem. Soc.*, 129 (2007), pp. 42–43.
5. R. Zeis et al., *J. Catalysis*, 253 (2008), pp. 132–138.
6. F. Yu et al., *Anal. Chem.*, 78 (2006), pp. 7346–7350.
7. P.N. Ciesielski et al., *ACS Nano*, 2 (2008), pp. 2465–2472.
8. N.E. Chayen et al., *J. Mol. Biol.*, 312 (2001), pp. 591–595.
9. ISI Web of Science, <http://apps.isiknowledge.com>.
10. A.J. Forty, *Nature*, 282 (1979), pp. 597–598.
11. C. Cennini, *The Craftsman's Handbook: The Italian "Il libro dell' arte"*, translated by Daniel V. Thompson, (New York: Dover Publications, 1960).
12. H.W. Pickering and C. Wagner, *J. Electrochem. Soc.*, 114 (1967), pp. 698–706.
13. J. Erlebacher, *J. Electrochem. Soc.*, 151 (2004), pp. C614–C626.
14. K. Sieradzki et al., *J. Electrochem. Soc.*, 149 (2002), pp. B370–B377.
15. K. Sieradzki et al., *Phil. Mag. A*, 59 (1989), pp. 713–746.
16. D.M. Artymowicz et al., *Phil. Mag.*, 89 (2009), pp.

- 1663–1693.
17. J. Rugolo et al., *Nature Materials*, 5 (2006), pp. 946–949.
18. A. Dursun et al., *Electrochem. and Solid State Lett.*, 6 (2003), pp. B32–B34.
19. P.G. Vekilov et al., *Acta Cryst.*, D58 (2002), pp. 1611–1616.
20. S. Ahl et al., *Plasmonics*, 3 (2008), pp. 13–20.
21. W.T. Zheng et al., *ASM Alloy Phase Diagrams Center*, editor-in-chief, P. Villars; section editors, H. Okamoto and K. Cenzual (Materials Park, OH: ASM International, 2006), [www.asminternational.org/AsmEnterprise/APD](http://www.asminternational.org/AsmEnterprise/APD).
22. Y. Sun and T.J. Balk, *Scripta Mat.*, 58 (2008), pp. 727–730.
23. C. Ji and P.C. Searson, *Appl. Phys. Lett.*, 81 (2002) pp. 4437–4439.
24. E. Seker et al., *Acta Mat.*, 56 (2008), pp. 324–332.
25. D. Lee et al., *Scripta Mat.*, 56 (2007), pp. 437–440.
26. N.A. Senior and R.C. Newman, *Nanotechnology*, 17 (2006), pp. 2311–2316.
27. Y. Ding et al., *Adv. Mat.*, 16 (2004), pp. 1897–1900.
28. F. Friedersdorf, “Stress-corrosion Cracking of Binary Noble Metal Alloys (Ph.D. thesis, Johns Hopkins University, 1994).
29. M. Hakamada and M. Mabuchi, *Nano Lett.* 6 (2006), pp. 882–885.
30. J. Weissmuller et al., *MRS Bulletin*, 34 (2009), pp. 577–586.
31. K. Sieradzki and R. Li, *Phys. Rev. Lett.*, 68 (1992), pp. 1168–1171.
32. D.J. Bailey and E.G. Brewer, *Metallurgical and Materials Trans. A*, 6 (1975), pp. 403–408.
33. J. Snyder and J. Erlebacher, *Langmuir*, 25 (2009), pp. 9596–9604.
34. J.W. Cahn et al., *Acta Mat.*, 54 (2006), pp. 4953–4975.
35. J.G. Velasco, *Chem. Phys. Lett.*, 313 (1999), pp. 7–13.
36. L.H. Qian and M.W. Chen, *Appl. Phys. Lett.*, 91 (2007), 083105.
37. A. Dursun et al., *J. Electrochem. Soc.* 150 (2003), pp. B355–B360.
38. P. Durkin and A.J. Forty, *Phil. Mag. A*, 45 (1982), pp. 95–105.
39. J. Snyder et al., *J. Electrochem. Soc.*, 155 (2008), pp. C464–C473.
40. J. Snyder et al., *Advanced Materials*, 20 (2008), pp. 4883–4886.
41. A.M. Hodge et al., *Adv. Eng. Mat.*, 8 (2006), pp. 853–857.
42. M. Hakamada and M. Mabuchi, *J. Mater. Res.*, 24 (2009), pp. 301–304.
43. J. Beiner et al., *J. Appl. Phys.* 97 (2005), 024301.
44. S. Van Petegem et al., *Nano Lett.*, 9 (2009), pp. 1158–1163.
45. J.C. Heyraud and J.J. Metois, *Acta Met.*, 28 (1980), pp. 1789–1797.
46. C. Herring, *The Physics of Power Metallurgy*, ed. W.E. Kingston (New York: McGraw-Hill, 1951), pp. 143–179.

**F. Kertis and J. Snyder are graduate students at Johns Hopkins University. L. Govada and S. Khurshid are in Prof. N. Chayen's group at Imperial College, London, U.K. J. Erlebacher, Professor of Materials Science and Engineering, and Chemical and Biomolecular Engineering at Johns Hopkins University, 3400 N. Charles St., Baltimore, MD 21218. Dr. Erlebacher can be reached at [Jonah.Erlebacher@jhu.edu](mailto:Jonah.Erlebacher@jhu.edu).**